Earthq Eng & Eng Vib (2014) 13: 509-518 **DOI**:10.1007/s11803-014-0258-5

A novel semi-active TMD with folding variable stiffness spring

M.H. Rafieipour[1†], A.K. Ghorbani-Tanha[2‡], M. Rahimian[2§] and R. Mohammadi-Ghazi[3,4†]

1. *Department of Civil Engineering, Science and Research Branch, Islamic Azad University, Tehran 39187-97717, Iran*
2. *School of Civil Engineering, College of Engineering, University of Tehran, P.O. Box 11155-4563, Tehran, Iran*
3. *Department of Civil and Environmental Engineering, Massachusetts Institute of Technology, Cambridge, MA, USA*
4. *Formerly with School of Civil Engineering, College of Engineering, University of Tehran, P.O. Box 11155-4563, Tehran, Iran*

Abstract: An innovative variable stiffness device is proposed and investigated based on numerical simulations. The device, called a folding variable stiffness spring (FVSS), can be widely used, especially in tuned mass dampers (TMDs) with adaptive stiffness. An important characteristic of FVSS is its capability to change the stiffness between lower and upper bounds through a small change of distance between its supports. This special feature results in lower time-lag errors and readjustment in shorter time intervals. The governing equations of the device are derived and simplified for a symmetrical FVSS with similar elements. This device is then used to control a single-degree-of-freedom (SDOF) structure as well as a multi-degree-of-freedom (MDOF) structure via a semi-active TMD. Numerical simulations are conducted to compare several control cases for these structures. To make it more realistic, a real direct current motor with its own limitations is simulated in addition to an ideal control case with no limitations and both the results are compared. It is shown that the proposed device can be effectively used to suppress undesirable vibrations of a structure and considerably improves the performance of the controller compared to a passive device.

Keywords: semi-active tuned mass damper; variable stiffness; folding variable stiffness spring

1 Introduction

Mass vibration absorbers are useful devices that are widely used to control undesirable vibrations in a variety of structures. One of the interesting absorbers of this kind is a tuned mass damper (TMD), which was first proposed by Frahm (1909). Although TMDs are theoretically high performance devices, they are not as efficient as they are designed. One of the main reasons is their sensitivity to tuning, which can be resolved to some extent by the use of active and hybrid counterparts. The active types of mass absorbers, active mass driver (AMD) and active tuned mass damper (ATMD), do not have the limitations of passive TMDs. However, the large power sources needed for their operation may not be available during a major excitation such as an earthquake. Moreover, most of the structures with active systems have a potential to be destabilized. These drawbacks are resolved in semi-active systems, which combine the best features of passive and active systems. In semi-active controllers, some of the mechanical properties of the system are changed based on a suitable control algorithm rather than applying force to some specific points (Housner *et al*., 1997; Yang *et al.*, 2005).

Semi-active TMDs (SATMDs) can be categorized based on their fundamental mechanical properties, which are mass, damping, and stiffness. Changing the mass of a device is not easy in most cases, although some studies have recently been done on this issue. Whirling-Beam Self-Tuning Vibration Absorber is another device that employs this concept (Ivres *et al*., 2008). In this device, asymmetric damping and stiffness on one side of a loosely threaded beam causes a moving mass to locate in an appropriate position; thus, the device readjusts automatically in real time. Mohammadi-Ghazi *et al*. (2012) proposed an innovative device that retunes by changing its configuration. In fact, changing the configuration of the device changes the mass moment of inertia that consequently regulates the device to a new condition. Another important tunable property is the damping of a TMD, which affects its damped frequency. Several studies have been conducted on this subject (Hrovat *et al*., 1983; Abe, 1996; Pinkaew and Fujino, 2001; Setareh, 2001 and 2002; Aldemir, 2003); however, such a tuning strategy is not very efficient

Correspondence to: M.H. Rafieipour, Department of Civil Engineering, Science and Research Branch, Islamic Azad University, Tehran, Iran
Tel: +98 2122342312; Fax: +98 2552221122
E-mail: mh.rafieipour@srbiau.ac.ir, rafieipour@gmail.com
[†]PhD Candidate; [‡]Assistant Professor; [§]Professor
Received March 9, 2013; **Accepted** March 19, 2014

for changing the tuning frequency. This is because the damped frequency of the device only slightly varies, even with a great change in its damping. The last property, stiffness, by which the device can be retuned, is much more efficient than changing the damping; that is why more studies have been focused on it. In fact, a broader frequency band can be covered by changing the stiffness. Several mechanisms with variable stiffness have been proposed such as the one by Walsh and Lamancusa (1992), which is made of two leaf springs. Another system was proposed by Nagarajaiah (2000), in which four springs were connected together to form a rhombus. The stiffness of the system varies by changing the aspect-ratio of the rhombus. Another system consisting of springs arranged in a circular configuration has also been proposed by Ghorbani-Tanha (2010). By rotating the rings on which the springs are connected, the configuration of the device and therefore its stiffness would change. Another example of such systems, proposed by Ghorbani-Tanha *et al*. (2011), works based on the unsymmetrical bending of a beam.

As stated before, all studies have been aimed at proposing a simpler mechanism with higher performance. One of the most important evaluation criteria of a controller is its ability to retune in a short period of time. The more rapidly the device retunes, the more favorable it is. The goal of this study is to propose a new novel variable stiffness system with a very simple mechanism that can be retuned much faster than most of its counterparts. In this system, stiffness change is accomplished by changing the length of a folding system. The mechanism is designed such that with slight changes in its tunable parameter, considerable changes in its stiffness can be achieved. Immediate readjustment capability, simplicity, and the broad frequency band coverage are the main advantages of this semi-active TMD with folding variable stiffness spring (FVSS).

2 General description of FVSS

FVSS is a combination of modular rhombuses which are made of beams with pinned connections (Fig. 1). The number of rhombuses can be varied based on the range of the stiffness required in each practical case for which the device is designed. In this study, it is considered that the load is in-plane and applied at the free end of the device. The stiffness of the free end of the device in the vertical direction is related to the mechanical properties of each element and also the geometry of the device. Moreover, as is shown in Fig. 1, it is obvious that the geometry of the device and hence its length changes if the distance between the supports varies. Consequently, such a strategy can be employed to change the effective stiffness of the free end of the device. Several mechanisms can be employed to change the distance between the supports in the vertical direction. For instance, a direct current (DC) motor with cables can be used to move them into a favorable position. Note that if both supports move

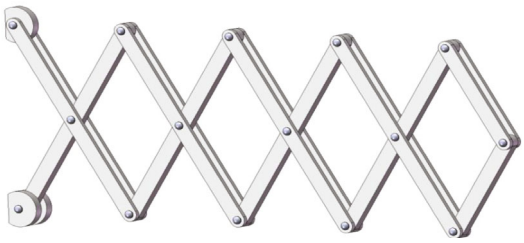

Fig. 1 General configuration of a FVSS (n = 9)

equally and symmetrically, the free end of the device moves in a horizontal direction. On the other hand, it is possible to change their position unequally or even change only the position of one support while the other remains fixed. In such cases, the free end of the FVSS moves both horizontally and vertically. The methodology to change the positions of the supports shown herein, affects the governing equations of the FVSS.

2.1 Governing equations

Two in-plane and one out-of-plane stiffness can be defined for this determinate system. The out-of-plane stiffness is considerably less than the in-plane stiffness due to the small moment of inertia corresponding to this direction, especially where the modular rhombuses are pinned together. Herein, the in-plane stiffness of the device, perpendicular to the moving direction of its free end, is calculated parametrically using the unit load method.

To simplify the equations, half of each rhombus is considered as a "module" that is connected together to form the device. Referring to Figs. 1 and 2, one it can be concluded that the number of these modules is always an odd integer. Thus, for a parametric study, it is assumed that there are n modules that form this structure where n is a natural, odd number. It is assumed that $n = 2N\text{-}1$ and the equations are derived using N.

The first two elements at the head, E_1^t and E_1^b, are rods with only axial force; however, the other elements are beam elements. The effect of axial force in the deflection of FVSS is not the same in different elements; in addition, some terms may be very small. However, the deflection of the device is calculated based on all these terms since an exact estimation of the stiffness is required in order to achieve acceptable results.

The downward deflection of the free end of the device, Point A, is comprised of three terms

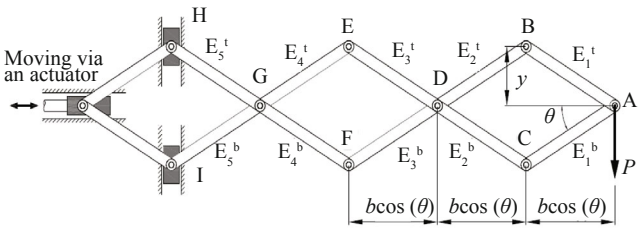

Fig. 2 Plane view of a FVSS with parametric properties (n = 5)

$$\Delta = \Delta_M + \Delta_V + \Delta_N \tag{1}$$

where Δ_M, Δ_V, and Δ_N are deflections caused by bending, shear, and axial force in all elements, respectively. Assuming all elements are identical in terms of material and cross section, each component of Eq. (1) can be derived as in Eq. (2). Note that the whole calculation is based on infinitesimal displacements. For a detailed derivation and simplification of these equations, see the Appendix.

$$\Delta_M = \frac{2}{9}\frac{Pb^3}{EI}N(N-1)(2N-1)\cos^2\theta \tag{2a}$$

$$\Delta_V = \frac{4}{3}\frac{Pf_s(1+\upsilon)}{EA}N(N-1)(2N-1)\cos^2\theta \tag{2b}$$

$$\Delta_N = \frac{Pb}{2EA\sin^2\theta}\left[2N\left[\frac{2}{3}(N-1)(2N-1)\cos^4\theta+1\right]-1\right] \tag{2c}$$

where P is the concentrated in-plane load, which is applied at Point A; E is the Young Modulus; υ is the Poisson's ratio; I is the moment of inertia of the cross section with respect to its principal axes perpendicular to the plane of device; A is the cross section area; f_s is the shear coefficient; θ is the angle of elements with respect to horizon; and b is the half length of the elements as shown in Fig. 2.

Using Eqs. (2), the stiffness of the system can be determined as a function of θ, which is

$$k(\theta) = \frac{\sin^2\theta}{\left[\alpha_1+\alpha_2\alpha_3\cot^2\theta\right]\cos^2\theta\sin^2\theta+\alpha_2(2N-1)} \tag{3}$$

in which

$$\alpha_1 = \frac{2N(N-1)(2N-1)}{3E}\left[\frac{b^3}{3I}+\frac{2f_s(1+\upsilon)}{A}\right],\ \alpha_2 = \frac{b}{2EA}$$

and $\alpha_3 = \frac{4}{3}N(N-1)(2N-1)$.

In practice, the required stiffness is calculated based on an appropriate control algorithm. The angle θ will then be modified in order to change the length of FVSS and obtain the appropriate stiffness needed. Changing the angle, θ, is equivalent to changing the distance between the supports, which is denoted by $2y$. Readjusting the device based on this distance seems to be much simpler than the angle θ. As a result, an appropriate distance between supports should be calculated based on a required stiffness. Noting that $\sin(\theta) = y/b$, Eq. (3) is solved parametrically for y. Four roots are obtained for y, which are

$$y_1 = \pm b\sqrt{\frac{2\beta_1}{\beta_2}};\qquad y_2 = \pm b\sqrt{-\frac{2\beta_1}{\beta_3}} \tag{4}$$

where β_1, β_2, and β_3 are as follows

$$\beta_1 = \alpha_2 k(2N-1+\alpha_3) \tag{5a}$$

$$\beta_2 = \left\{\alpha_1 k\left[\alpha_1 k-4\alpha_2 k(2N-1)-2\right]+4\alpha_2\alpha_3 k\left[1-\alpha_2 k(2N-1)\right]+1\right\}^{\frac{1}{2}} - \alpha_1 k+2\alpha_2\alpha_3 k+1 \tag{5b}$$

$$\beta_3 = \left\{\alpha_1 k\left[\alpha_1 k-4\alpha_2 k(2N-1)-2\right]+4\alpha_2\alpha_3 k\left[1-\alpha_2 k(2N-1)\right]+1\right\}^{\frac{1}{2}} + \alpha_1 k-2\alpha_2\alpha_3 k-1 \tag{5c}$$

The only acceptable root is the one that is real and positive.

A very important characteristic of this device, which makes it different from its counterparts, is the relation between the rate of change of the length of the device and the distance between its supports. Considering L as the length of the FVSS, it can be stated that

$$L = n\sqrt{b^2-y^2} \tag{6}$$

Differentiating Eq. (6) with respect to y shows the relation between these rates as

$$\left|\frac{\mathrm{d}L}{\mathrm{d}y}\right| = ny/\sqrt{b^2-y^2} \tag{7}$$

In other words, by changing y, the length of FVSS changes by the scale factor of ny. In fact, little variation in y results in considerable change in the length of the device. Therefore, readjustment of the device can be accomplished much faster than its counterparts. Note that y usually does not take very small values in practice.

There are different ways to connect the FVSS to a TMD to make an SATMD. One of the possible ways is schematically shown in Fig. 3.

Note that all these equations are derived for a FVSS in which the capacity for axial force, shear, and bending of all elements are equal. Therefore, its design may not be optimum, since the elements in different positions are of different forces. However, such an assumption makes the formulation very easy and simple.

2.2 Numerical examples

The efficacy of the proposed FVSS is evaluated via numerical examples. A very simple excitation has been considered in these examples to avoid the complications of excitation effects. Thus, the performance of the device

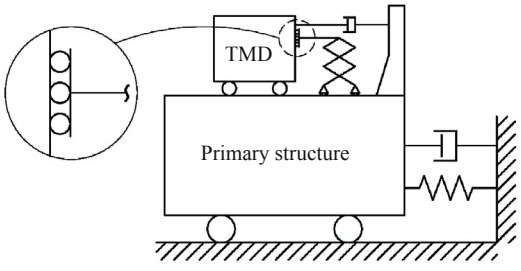

Fig. 3 A possible form for connecting a FVSS to a TMD

can be evaluated more precisely. The excitation simulates the vibrations produced by a rotating unbalance mass m_{ub} and eccentricity of R whose frequency varies according to Fig. 4. This excitation simulates the vibrations produced by the rotating machine during the start-up period and can be defined as (Walsh and Lamancusa, 1992)

$$f(t)=\begin{cases} m_{ub}R(\alpha t)^2\sin(\dfrac{\alpha t^2}{2})-m_{ub}R\alpha\cos(\dfrac{\alpha t^2}{2}), & t<t_{acc} \\ m_{ub}R\omega_{max}^2\sin(\omega_{max}t), & t\geq t_{acc} \end{cases} \tag{8}$$

where α is the angular acceleration of the rotating unbalance; t_{acc} is the time at which the acceleration ends; and ω_{max} is the operating frequency. The maximum frequency of the excitation is equal to the natural frequency of the structure, so the performance of the device is evaluated for the case of resonance, which is the most critical condition.

As the first example, a SDOF structure is considered as the primary structure that should be controlled. The excitation parameters are taken as , m_{ub} = 1 kg, R = 0.2 m , t_{acc} = 2 s, α = 20π rad/s^2, and ω_{max} = 40π rad/s^2. The performance of the semi-active device is compared to a passive TMD's. The properties of the SDOF structure, along with the passive and semi-active TMDs, are listed in Table 1.

In the next example, the device is used to control a MDOF structure. The excitation parameters are taken as m_{ub} = 1 kg, R = 0.2 m , t_{acc} = 2 s, α = 10π rad/s^2, and ω_{max} = 20π rad/s^2. The MDOF structure was studied by Chung *et al.* (1989) and has the modal frequencies of 2.24, 6.83, and 11.53 Hz, respectively. As is observed, the first two modes' frequencies are very different from

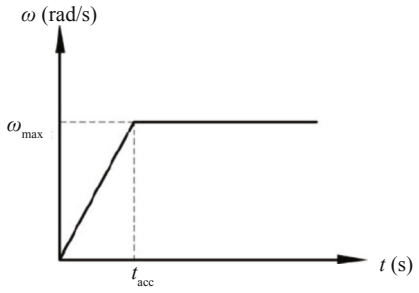

Fig. 4 Frequency of excitation

the maximum frequency of the excitation, i.e., ω_{max} = 20π rad/s^2; therefore, resonance does not occur by the mentioned excitation. Hence, in the present study, the stiffness and damping matrices are taken to be the same as those of Chung *et al*. (1989), but the mass matrix of the structure is scaled by a factor of 0.05. The mass, stiffness, and damping matrices for the simulated MDOF structure are, respectively, as follows

$$\boldsymbol{M}=\begin{bmatrix} 50.12 & 0 & 0 \\ 0 & 50.12 & 0 \\ 0 & 0 & 50.12 \end{bmatrix}(\text{kg});$$

$$\boldsymbol{K}=\begin{bmatrix} 2.8012 & -1.6772 & 0.3772 \\ -1.6772 & 3.0878 & -1.6600 \\ 0.3772 & -1.6600 & 1.3625 \end{bmatrix}\times 10^6(\text{N/m});$$

$$\boldsymbol{C}=\begin{bmatrix} 391.115 & -58.533 & 63.008 \\ -58.533 & 466.832 & -2.865 \\ 63.008 & -2.865 & 446.963 \end{bmatrix}(\text{N}\cdot\text{s/m})$$

Table 1 Properties of the SDOF structure, passive TMD and SATMD

Structure		TMD		SATMD with FVSS	
M_s^* (kg)	1000	M_{TMD}^* (kg)	50	M_{SATMD}^* (kg)	50
ω_n (rad/s)	40π	ω_n (rad/s)	40π	k_{max} * (N/m)	1.18×10^8
ζ_s^*	0.05	ζ_{TMD}^*	0.02	k_{min} * (N/m)	3.61×10^5
				ζ_{SATMD}^*	0.02
				θ_{max}	75°
				θ_{min}	5°
				n	7
				α_1	9.39×10^{-7}
				α_2	1.19×10^{-10}
				α_3	112

*M, ζ , and k are, respectively, representative of mass, damping ratio, and stiffness. The subscripts s, TMD, and SATMD indicate the system for which the properties are defining.

The modal frequencies of the new MDOF structure are 10.00, 30.43, and 51.37 Hz, respectively. It is obvious that the frequency of the first mode becomes equal to the maximum excitation frequency. Moreover, the excitation is applied to the first floor of the structure.

Like the SDOF structure, the performance of the semi-active device is compared to a passive TMD for the MDOF structure. The properties of the TMD and SATMD used to control the MDOF structure are presented in Table 2.

2.3 Control algorithms

Since the properties of the structures and excitation are already known, an open loop control algorithm based on instantaneous frequency of excitation is used in this example. This algorithm prevents some of the undesirable effects such as errors in the calculation of instantaneous frequency ordue to time-delay. This in turn makes it possible to focus on the performance of the device itself.

In this algorithm, it is assumed that the natural frequency of the device is equal to the instantaneous frequency of the excitation. Denoting the excitation frequency by $\omega(t)$ and the mass of the absorber by m_{va}, the required stiffness is calculated as

$$k_{req}(\theta) = m_{va}\omega^2(t) \tag{9}$$

Adding $k_{req}(\theta)$ in Eqs. (4) and (5), the required distance between the supports of FVSS, y_{req}, is determined. Due to geometrical constraints, y cannot assume every desirable value, so the algorithm is expressed with its general constraints as

$$y = \min\left[y_{max}, \max\left(y_{min}, y_{req}\right)\right] \tag{10}$$

where y_{max} and y_{min} are the upper and lower bounds for y, respectively.

Although this algorithm shows the theoretical performance of the device, it may not be feasible in practice due to limitations in velocity or the applied torque of DC motors, etc. In other words, it is not generally possible for the supports to be instantaneously re-arranged in a favorable position even if instantaneous frequency is exactly derived. For instance, if the excitation is generated during the start-up of a rotary machine, the instantaneous frequency is known; however, in the case of high angular acceleration of the machine, the velocity of FVSS's supports may exceed the limit of their drivers. Hence, the readjustment may not be perfectly achieved even in open loop systems. To investigate the efficacy of the device in such conditions, another control case is simulated in which a real DC motor is modeled for each of the structures. Note that both control cases are based on the instantaneous frequency of the excitation and the only difference is that in the second case, the limitations of a real DC motor are being considered.

The considered DC motors in this study are permanent magnet motors for which there is a linear relation between torque and rpm for a given voltage. The maximum torque at zero rpm is called *stall torque* and zero torque occurs at maximum rpm, which is called *free rpm*. The relation between the torque, T, and a given rpm, R, is

$$T = T_s\left(1 - \frac{R}{R_f}\right) \tag{11}$$

where T_s and R_f are stall torque and free rpm, respectively. The properties of the DC motors for each of the SDOF and MDOF structures are presented in Table 3.

2.4 Evaluation criteria

Six non-dimensional evaluation criteria are defined to compare the performance of the semi-active TMD in

Table 2 Properties of the passive TMD and SATMD for the MDOF structure

TMD		SATMD with FVSS	
M_{TMD} (kg)	3.5	M_{SATMD} (kg)	3.5
ω_n (rad/s)	20π	k_{max}(N/m)	2.96×10^5
ζ_{TMD}	0.02	k_{max}(N/m)	2.40×10^3
		ζ_{SATMD}	0.02
		θ_{max}	75°
		θ_{min}	5°
		n	7
		α_1	4.18×10^{-4}
		α_2	1.19×10^{-10}
		α_3	112

Table 3 Properties of DC motors

Property	SDOF structure	MDOF structure
Voltage	12	12
T_s (kg·cm)	40	27
R_f (rpm)	50	800
Rotor diameter (m)	0.02	0.012

reducing systems' responses with a passive TMD. Three evaluation criteria are based on maximum responses and the next three are defined by normed system responses [Root Mean Square (RMS)].These evaluation criteria are

$$J^{s}_{d-\max}=\frac{\max\left|x_{s}^{\mathrm{SATMD}}\right|}{\max\left|x_{s}^{\mathrm{TMD}}\right|} \tag{12}$$

$$J^{s}_{v-\max}=\frac{\max\left|\dot{x}_{s}^{\mathrm{SATMD}}\right|}{\max\left|\dot{x}_{s}^{\mathrm{TMD}}\right|} \tag{13}$$

$$J^{s}_{a-\max}=\frac{\max\left|\ddot{x}_{s}^{\mathrm{SATMD}}\right|}{\max\left|\ddot{x}_{s}^{\mathrm{TMD}}\right|} \tag{14}$$

$$J^{s}_{d-\mathrm{RMS}}=\frac{\left\|x_{s}^{\mathrm{SATMD}}\right\|}{\left\|x_{s}^{\mathrm{TMD}}\right\|} \tag{15}$$

$$J^{s}_{v-\mathrm{RMS}}=\frac{\left\|\dot{x}_{s}^{\mathrm{SATMD}}\right\|}{\left\|\dot{x}_{s}^{\mathrm{TMD}}\right\|} \tag{16}$$

$$J^{s}_{a-\mathrm{RMS}}=\frac{\left\|\ddot{x}_{s}^{\mathrm{SATMD}}\right\|}{\left\|\ddot{x}_{s}^{\mathrm{TMD}}\right\|} \tag{17}$$

where x_s^{SATMD} and x_s^{TMD} are the displacement response of the structure controlled by a variable stiffness TMD and a passive TMD, respectively. A dot represents the derivative with respect to time. The norm $\|\,.\,\|$ is the RMS of responses; $|\,.\,|$ is the absolute value; subscripts *d*, *v*, and *a*, respectively, represent the criteria for the comparison of the displacement, velocity, and acceleration responses.

3 Results and commentary

The roof displacement responses of the SDOF and MDOF structures due to external excitation applied to the first floor are shown in Figs. 5 and 6, respectively. To be concise, the other responses are not shown in separate figures and are only compared based on the evaluation criteria. The variations of *y* for both structures are shown in Fig. 7. As shown in Figs. 5 and 6, simulating a real motor has a considerable effect on the response of SDOF structure; whereas it does not substantially affect the response of the MDOF structure. One important reason is that the MDOF structure has a lower frequency of excitation since the TMDs' performance are higher in low frequencies; thus, the behavior of passive and semi-active TMDs with the ideal algorithm or the real motor are closer in such cases. Another reason is that the semi-active TMD with a real motor is adjusted to the excitation after the acceleration time. In contrast, the device with a real motor is adjusted to the excitation before the acceleration time is met in the case of the MDOF structure (Fig. 7). In other words, the control device of the MDOF structure is not matched to the vibration only at its beginning, which does not have a significant contribution to the behavior of the structure. Whereas, the controller fails to be matched to the excitation, mostly during the accelerating period, in the case of the SDOF structure. Thus, its behavior is not similar to the ideal controller.

Additional comparisons between different cases are presented in Tables 4 and 5, which lists evaluation criteria for SDOF and MDOF structures, respectively. Based on these results, it is concluded that the semi-active TMD with an ideal algorithm has the best performance. The semi-active TMD with a real motor, despite having lower performance in comparison with the ideal one, suppresses the response of the structures considerably more than the passive TMD. As it was stated before, the difference between the ideal algorithm and real motor is negligible in the MDOF structure.

A parametric study is conducted to investigate the performance of the proposed SATMD under a variety of transient vibrations with different angular acceleration. The MDOF structure's responses are obtained for various values of angular accelerations of the rotating unbalance. For each case, all the excitation parameters except α and hence $\omega_{\max}$, because $\omega_{\max}=\alpha\, t_{\mathrm{acc}}$, are taken to be constant and the same as presented in Table 2. Because the SATMD should be compared with an appropriate TMD for every case, the TMD is adjusted with the excitation operating

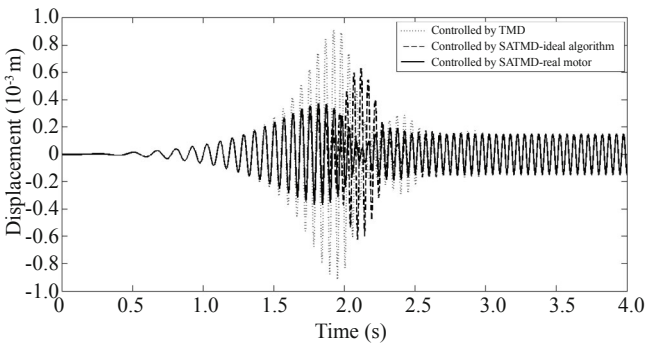

Fig. 5 Roof displacement response of SDOF structure

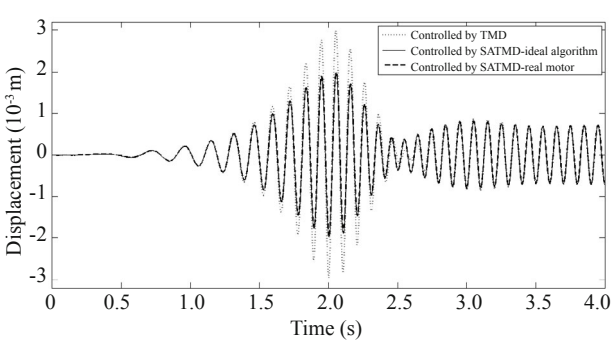

Fig. 6 Roof displacement response of MDOF Structure

Table 4 Evaluation criteria for SDOF structure

	$J^s_{d-\max}$	$J^s_{v-\max}$	$J^s_{a-\max}$	$J^s_{d-\mathrm{RMS}}$	$J^s_{v-\mathrm{RMS}}$	$J^s_{a-\mathrm{RMS}}$
Ideal algorithm	0.40	0.39	0.38	0.57	0.58	0.59
Real motor	0.69	0.74	0.79	0.69	0.73	0.78

Table 5 Evaluation criteria for MDOF structure

		$J^s_{d-\max}$	$J^s_{v-\max}$	$J^s_{a-\max}$	$J^s_{d-\mathrm{RMS}}$	$J^s_{v-\mathrm{RMS}}$	$J^s_{a-\mathrm{RMS}}$
Ideal algorithm	Story 1	0.664	0.668	0.673	0.765	0.770	0.777
	Story 2	0.664	0.668	0.673	0.764	0.768	0.775
	Story 3	0.663	0.667	0.673	0.763	0.767	0.773
Real motor	Story 1	0.663	0.666	0.672	0.763	0.768	0.775
	Story 2	0.662	0.666	0.672	0.762	0.767	0.774
	Story 3	0.662	0.666	0.671	0.762	0.765	0.772

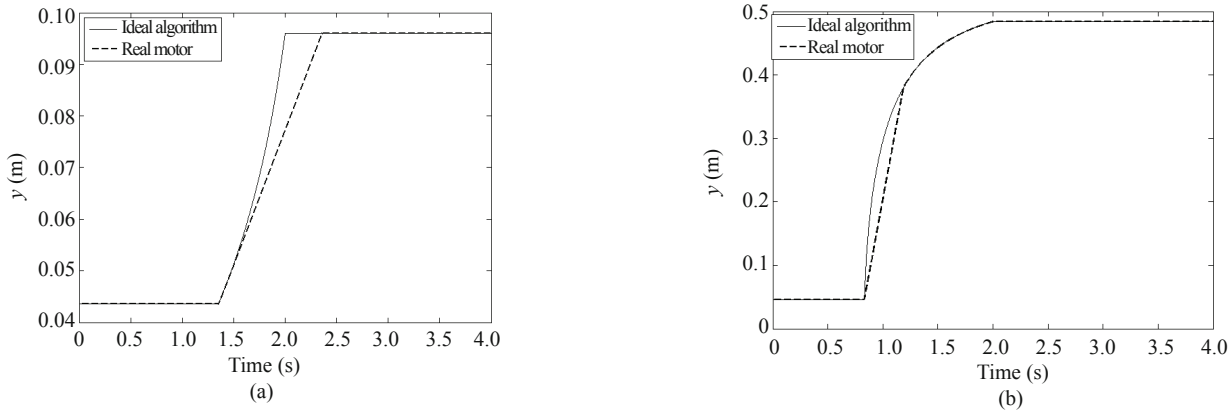

Fig. 7 Variation of *y* for: (a) SDOF structure; (b) MDOF structure

frequency for each transient vibration by changing its stiffness. The variations of $J^s_{d-\max}$ and $J^s_{d-\mathrm{RMS}}$ versus α are presented in Figs. 8 and 9, respectively. These figures show that SATMD is more effective for higher values of angular acceleration of the excitation.

Another important result is the variation of each component of Eq. (1) versus *y*. This result can help in the design of the FVSS; since for some values of *y,* the elements' moment may control the design of the device while for some other values of *y,* the axial force may do so. The variation of each component vs. *y* for SDOF and MDOF structures is illustrated in Figs.10 and 11, respectively. In both structures, Δ_V is not a considerable portion of the total deformation of FVSS, since none of its components nor the device as a whole are like a shear beam. On the other hand, Δ_N is comparable to Δ_M in the case of the SDOF structure although its contribution in the deflection of the device is negligible in the case of the MDOF structure. This is because their geometries are different and their axial and bending stiffnesses are of a different order.

Another important result is the variations of the torque applied by the DC motor to the supports of the FVSS. This result is shown in Fig. 12 for both SDOF and MDOF structures.

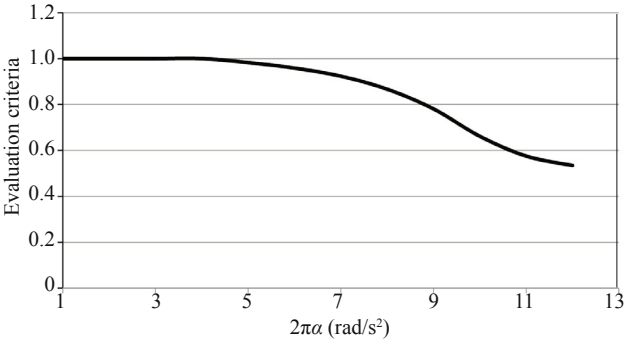

Fig. 8 Variations of $J^s_{d-\max}$ versus α

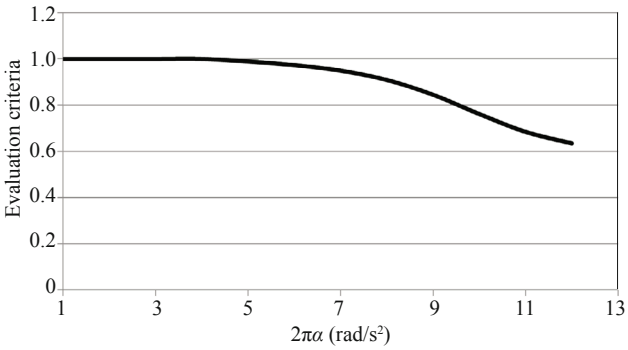

Fig. 9 Variations of $J^s_{d-\mathrm{RMS}}$ versus α

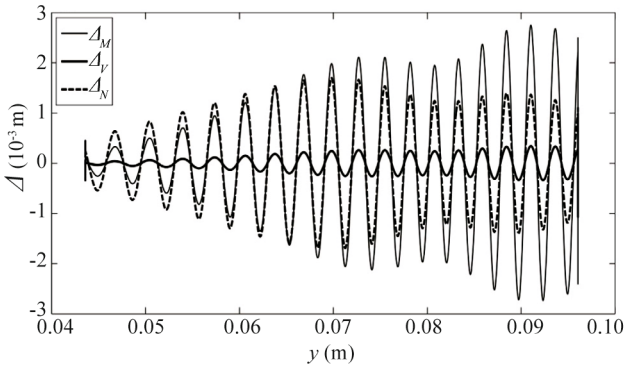

Fig. 10 Variation of Δ_M, Δ_V, and Δ_N vs. y for SDOF structure

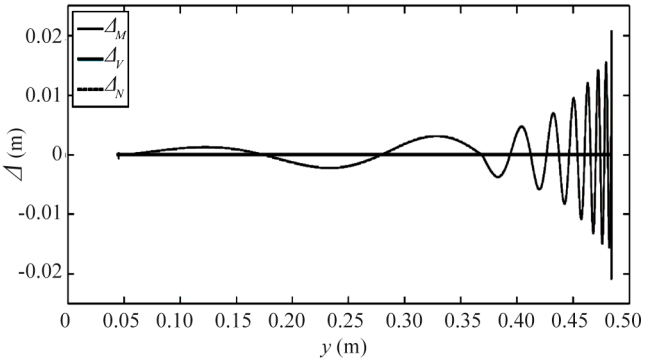

Fig. 11 Variation of Δ_M, Δ_V, and Δ_N vs. y for MDOF structure

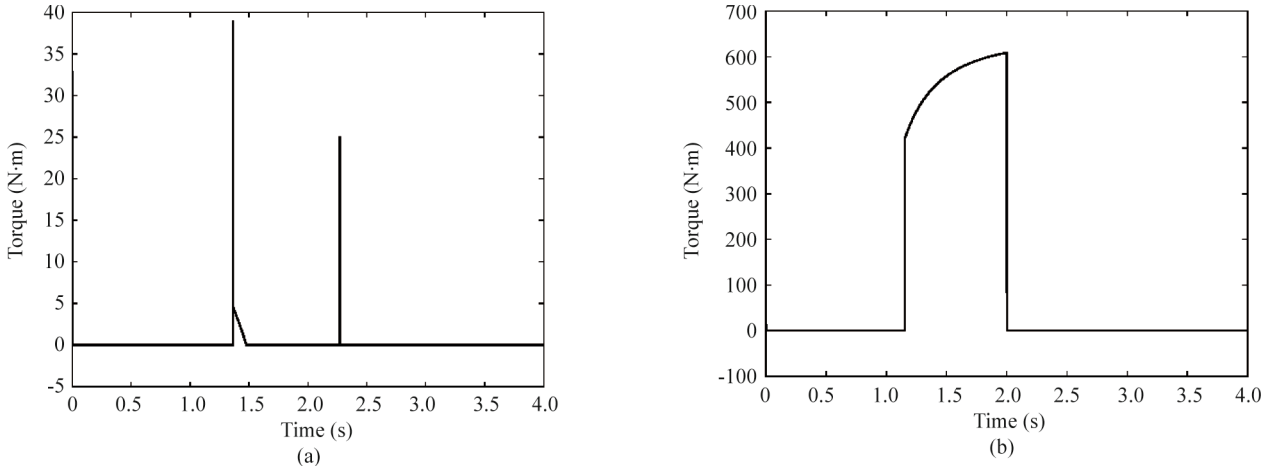

Fig. 12 Variations of the torque applied by DC motor to the supports of FVSS: (a) SDOF; (b) MDOF

4 Conclusions

A new variable stiffness device is proposed and investigated by using in a semi-active TMD. The stiffness of the device changes by changing its length and geometry. The rate of adjustment in this device varies based on its length in each time-step and it can be readjusted much faster for the lower frequencies. Numerical examples for SDOF and MDOF structures were conducted and the results demonstrated that the proposed device can significantly suppress the undesirable vibrations of the structures.

To make the examples more realistic, two control cases for each structure were considered. For the first case, an ideal control algorithm was employed which had no limitation in readjustment rate, velocity of supports, and type of drivers. The only constraint in this case was the lower and upper bounds of y. In the second case, a real DC motor was simulated with specific values for maximum torque and rpm for each structure. The results of the simulations show that despite lower performance in the second case with a real motor, the semi-active TMD with FVSS mitigates the vibrations for SDOF and MDOF structures more than 30% and 22%, respectively, compared to a passive TMD. Note that a control algorithm based on instantaneous frequency was used here with no error in calculation of the excitation's frequency. Thus, the example is appropriate for cases where the excitation is completely known in advance and it is reasonable to use an open-loop control strategy. For the other cases, it is recommended to use some other algorithms such as Proportional-Integral-Derivative (PID).

Another important result that is essential in the design of a FVSS is the variation of each component of its deformation. It can be concluded based on the results that shear force does not have a considerable impact on the design of the device. On the other hand, axial force may determine the design and as is obvious, the only criteria for the first two elements at the head of a FVSS are the axial force, since they are truss elements.

Acknowledgement

The authors wish to express their sincere gratitude to Dr. M.T. Mahyari for his help in editing the manuscript.

References

Abe M (1996), "Semi-active Tuned Mass Dampers for Seismic Protection of Civil Structures," *Journal of Earthquake Engineering and Structural Dynamics*, **25**(7): 743−749.

Aldemir U (2003), "Optimal Control of Structures with Semiactive-tuned Mass Dampers," *Journal of Sound and Vibration*, **266**(4): 847−874.

Chung LL, Lin RC, Soong TT and Reinhorn AM (1989), "Experimental Study of Active Control for MDOF Seismic Structures," *Journal of Engineering Mechanics*, **115**(8): 1609−1627.

Frahm H (1909), "Device for Damping Vibrations of Bodies," *US Patent No. 989,958*, October 30, 1909.

Ghorbani-Tanha AK (2010), "Development of a Novel Semi-active Tuned Mass Damper for Vibration Control of Structures," *5th World Conference on Structural Control and Monitoring*, 12−14 July, Tokyo, Japan, Paper No. 125.

Ghorbani-Tanha AK, Rahimian M and Noorzad A (2011), "A Novel Semi-active Variable Stiffness Device and Its Application in a New Semi-active Tuned Vibration Absorber," *Journal of Engineering Mechanics*, **137**(6): 390−400.

Housner GW, BergmanVT, Caughey K,Chassiakos AG, Claus SF, Masri RO, Skelton RE, Soong TT, Spencer Jr BF and Yao JTP (1997), "Structural Control: Past, Present, and Future," *Journal of Engineering Mechanics*, **123**(9): 897−971.

Hrovat D, Barak P and Rabins M (1983), "Semi-active Versus Passive or Active Tuned Mass Dampers for Structural Control," *Journal of Engineering Mechanics*, **109**(3): 691−705.

Ivers D, Wilson R and Margolis D (2008), "Whirling-Beam Self-tuning Vibration Absorber," *Journal of Dynamic Systems, Measurement, and Control*, **130**(3): Art. No. 031009.

Mohammadi-Ghazi R, Ghorbani-Tanha AK and Rahimian M (2012), "Adaptive Configuration Tuned Mass Damper for Mitigation of Rotational Vibrations," *Journal of Engineering Mechanics*, **138**(8): 934−944.

Nagarajaiah S (2000), "Structural Vibration Damper with Continuously Variable Stiffness", *US Patent No. 6,098,969*, Aug. 8, 2000.

Pinkaew T and Fujino Y (2001), "Effectiveness of Semi-active Tuned Mass Damper under Harmonic Excitation," *Journal of Engineering Structures*, **23**(7): 850−856.

Setareh M (2001), "Application of Semi-active Tuned Mass Dampers to Base-excited systems," *Journal of Earthquake Engineering and Structural Dynamics*, **30**(3): 449−462.

Setareh M (2002), "Floor Vibration Control Using Semi-active Tuned Mass Dampers," *Canadian Journal of Civil Engineering*, **29**(1): 76−84.

Walsh PL and Lamancusa JS (1992), "A Variable Stiffness Vibration Absorber for Minimization of Transient Vibrations," *Journal of Sound and Vibration*, **158**(2): 195−211.

Yang YB, Lu LY and Yau JD In: de Silva CW, Editor (2005), *Vibration and Shock Handbook*, CRC Press, Taylor & Francis Group, Boca Raton, Florida.

Appendix

In this part, the procedure of analyzing the structure and simplifications of the equations are stated. The Unit Load Method is employed to calculate each component of Eq. (1). Before the calculation of the mentioned components, the structure should be analyzed. For simplicity, each element is named as E_i^t or E_i^b where $i = 1,2,\ldots N$ (Fig. 2). The superscript t indicates that the element is at the top of the axis of the device and the superscript b indicates that the element is at the bottom of the axis. The subscript i indicates the number of module (half rhombus), beginning from Point A, at which the element is located. For example, E_3^t is the element at the third module from Point A, which is located at the top of the axis of the device. It is obvious that the maximum of i is n. It should be noted that the axis of the device is a horizontal line which crosses Point A (Fig. 2) and perpendicular to the line which crosses both supports. Although all elements, except the first two elements which are connected to Point A, are continuous at the intersection point with other elements, each part of them is called with a different name. For instance, the element between the Point B and F is continuous and pinned with another element at Point D; nevertheless, the first part which is BD is called E_2^t and the second part which is DF is called E_2^b. The reason is that the shear and axial forces of each part are constant through its length and different from the other part.

Before analyzing, it should be noted that in each time step, the supports are considered to be fixed; thus, the device can be statically analyzed. The element E_1^t and E_1^b are truss elements and the FVSS is a determinate structure. The axial force, shear, and moment of each element are denoted by N_i^t , V_i^t, and M_i^t, respectively. Assuming force P is applied to point A, one can conclude that N_i^t and V_i^t can be determined based on their subscript which can be odd or even. Thus, it is obtained that

$$N_i^t = \frac{P}{2\sin\theta}\left[(i-1)\cos^2\theta - 1\right]$$
$$N_i^b = -\frac{P}{2\sin\theta}\left[(i-1)\cos^2\theta - 1\right] \quad ; \quad i \text{ is odd} \qquad \text{(A1)}$$
$$V_i^t = V_i^b = \frac{(i-1)}{2}P\cos\theta$$

$$N_i^t = \frac{P}{2\sin\theta}\left[i\cos^2\theta + 1\right]$$
$$N_i^b = -\frac{P}{2\sin\theta}\left[i\cos^2\theta + 1\right] \quad ; \quad i \text{ is even} \qquad \text{(A2)}$$
$$V_i^t = V_i^b = -\frac{i}{2}P\cos\theta$$

For a continuous system, the Unit Load Method is stated as

$$\Delta = \int_L \frac{M \cdot m}{EI} \mathrm{d}x + \int_L \frac{N_\mathrm{a} \cdot n}{EA} \mathrm{d}x + \int_L f_\mathrm{s} \frac{V \cdot v}{GA} \mathrm{d}x \qquad \text{(A3)}$$

where Δ is the displacement in direction of the unit load; G is the shear modulus; m, n, and v are the moment, axial force, and the shear of the system with the unit load; M, N_a, and V are the moment, axial force, and the shear of the system with force P. For a system with n elements and constant internal forces in each element, Eq. (A3) can be stated as

$$\Delta = 2\left[\sum_{i=1}^{n} \frac{M_i \cdot m_i}{E_i I_i} + \sum_{i=1}^{n} \frac{N_{\mathrm{a},i} \cdot n_i}{E_i A_i} + \sum_{i=1}^{n} f_{\mathrm{s},i} \frac{V_i \cdot v_i}{G_i A_i}\right] \qquad \text{(A4)}$$

The first term of Eq. (A4) is Δ_M, the second one is Δ_N, and the third one is Δ_V. Assuming that all elements of FVSS are identical and using (A1), (A2), and (A4) one can obtain

$$\Delta_M = \frac{4}{3} \frac{Pb^3}{EI} \cos^2\theta \sum_{j=1}^{N} (j-1)^2 \qquad \text{(A5)}$$

$$\Delta_V = \frac{4Pf_\mathrm{s}}{GA} \cos^2\theta \sum_{j=1}^{N} (j-1)^2 \qquad \text{(A6)}$$

$$\Delta_N = \frac{Pb}{2EA\sin^2\theta}\left[1 + \left(2\cos^2\theta - 1\right)^2 + \left(2\cos^2\theta + 1\right)^2 + \ldots + \left(2(N-1)\cos^2\theta + 1\right)^2\right] \qquad \text{(A7)}$$

Knowing that for natural number r $\sum_{s=0}^{r} s^2 = \sum_{s=1}^{r} s^2 = \frac{r(r+1)(2r+1)}{6}$, $G = \frac{E}{2(1+\upsilon)}$, and expansion of each term of (A7), Eqs. (A5) to (A7) are simplified as

$$\Delta_M = \frac{4}{3} \frac{Pb^3}{EI} \frac{N(N-1)(2N-1)}{6} \cos^2\theta \qquad \text{(A8)}$$

$$\Delta_V = \frac{8Pf_\mathrm{s}}{EA}(1+\nu) \frac{N(N-1)(2N-1)}{6} \cos^2\theta \qquad \text{(A9)}$$

$$\Delta_N = \frac{Pb}{2EA\sin^2\theta}\left[2N\left[\frac{2}{3}(N-1)(2N-1)\cos^4\theta + 1\right] - 1\right] \qquad \text{(A10)}$$

The summation of Eqs. (A8) to (A10) and also defining the constants α_1, α_2, and α_3 gives the total displacement of the FVSS at point A that is

$$\Delta = P\left[\left(\alpha_1 + \alpha_2\alpha_3 \cot^2\theta\right)\cos^2\theta + \frac{\alpha_2}{\sin^2\theta}(2N-1)\right] \qquad \text{(A11)}$$

In order to obtain the mentioned stiffness, Δ in Eq. (A11) is taken as unity and the equation is solved for P. The obtained result for P which is a function of θ is called the stiffness of FVSS at point A in the direction of P (Eq. (3)).